

## Study of negative thermal expansion in the frustrated spinel $\text{ZnCr}_2\text{Se}_4$

X. L. Chen, Z. R. Yang, W. Tong, Z. H. Huang, L. Zhang, S. L. Zhang, W. H. Song, L. Pi, Y. P. Sun, M. L. Tian, and Y. H. Zhang

Citation: *Journal of Applied Physics* **115**, 083916 (2014); doi: 10.1063/1.4867217

View online: <http://dx.doi.org/10.1063/1.4867217>

View Table of Contents: <http://scitation.aip.org/content/aip/journal/jap/115/8?ver=pdfcov>

Published by the [AIP Publishing](#)

---

### Articles you may be interested in

[Pressurizing the  \$\text{HgCr}\_2\text{Se}\_4\$  spinel at room temperature](#)

*Appl. Phys. Lett.* **104**, 011911 (2014); 10.1063/1.4861591

[Low-dilution limit of  \$\text{Zn}\_1 \times \text{Mn}\_x \text{GeAs}\_2\$ : Electrical and magnetic properties](#)

*J. Appl. Phys.* **114**, 093908 (2013); 10.1063/1.4820475

[Correlations, spin dynamics, defects: the highly frustrated kagomé bilayer](#)

*Low Temp. Phys.* **31**, 704 (2005); 10.1063/1.2008131

[Magnetic frustration in the spinel compounds  \$\text{Ge Ni}\_2 \text{O}\_4\$  and  \$\text{Ge Co}\_2 \text{O}\_4\$](#)

*J. Appl. Phys.* **97**, 10A512 (2005); 10.1063/1.1863113

[Influence of a nonmagnetic dilution on the magnetic properties of a  \$\text{Zn}\_x \text{Cd}\_{1-x} \text{Cr}\_2 \text{S}\_4\$  system by means of microwave magnetic resonance](#)

*J. Appl. Phys.* **97**, 10A507 (2005); 10.1063/1.1852854

---



**AIP** | Journal of Applied Physics

*Journal of Applied Physics* is pleased to announce **André Anders** as its new Editor-in-Chief

## Study of negative thermal expansion in the frustrated spinel $\text{ZnCr}_2\text{Se}_4$

X. L. Chen,<sup>1</sup> Z. R. Yang,<sup>1,a)</sup> W. Tong,<sup>2</sup> Z. H. Huang,<sup>2</sup> L. Zhang,<sup>2</sup> S. L. Zhang,<sup>2</sup> W. H. Song,<sup>1</sup> L. Pi,<sup>2,3</sup> Y. P. Sun,<sup>1,2</sup> M. L. Tian,<sup>2</sup> and Y. H. Zhang<sup>2,3</sup>

<sup>1</sup>Key Laboratory of Materials Physics, Institute of Solid State Physics, Chinese Academy of Sciences, Hefei 230031, People's Republic of China

<sup>2</sup>High Magnetic Field Laboratory, Chinese Academy of Sciences, Hefei 230031, People's Republic of China

<sup>3</sup>University of Science and Technology of China, Hefei 230026, People's Republic of China

(Received 17 January 2014; accepted 18 February 2014; published online 28 February 2014)

The origin of negative thermal expansion (NTE) in the bond frustrated  $\text{ZnCr}_2\text{Se}_4$  has been explored. ESR and FTIR document an ideal paramagnetic state above 100 K, below which ferromagnetic clusters coexist with the paramagnetic state down to  $T_N$ . By fitting the inverse susceptibility above 100 K using a modified paramagnetic Curie-Weiss law, an exponentially changeable exchange integral  $J$  is deduced. In the case of the variable  $J$ , magnetic exchange and lattice elastic energy couple with each other effectively via magnetoelastic interaction in the ferromagnetic clusters, where NTE occurs at a loss of exchange energy while a gain of lattice elastic one. © 2014 AIP Publishing LLC. [<http://dx.doi.org/10.1063/1.4867217>]

### I. INTRODUCTION

Magnetic frustrated systems have recently been a subject of continuing interests for a manifold of fascinating states, such as spin ice, spin liquid, and orbital glass, may be surviving down to  $T=0$ .<sup>1-3</sup> Among the reported materials, chromium-based spinels with the formula  $\text{ACr}_2\text{X}_4$  ( $X = \text{O}, \text{S},$  and  $\text{Se}$ ) are of essential role not only of being theoretical interests but also in exploring potential multi-functional materials.<sup>4-7</sup> For instance, magnetoelectric effect or multiferroicity is observed in  $\text{ZnCr}_2\text{Se}_4$ .<sup>8,9</sup> In addition, it allows the adjustments of the direction and magnitude of electric polarization via applied magnetic field.<sup>9</sup> The design or tuning of multi-functional materials for potential applications enables the necessity to clear what stands behind the novel phenomena observed.

$\text{ZnCr}_2\text{Se}_4$  with negative thermal expansion (NTE) is a case in point.<sup>6,10</sup> This compound exhibits a large positive Curie-Weiss temperature.<sup>11</sup> However, neutron diffraction study revealed at  $T_N=21$  K a complex helical spins consisted of ferromagnetic (FM) layers along [001] with a turning angle of  $42^\circ$  between the adjacent ones.<sup>12-14</sup> While early X-ray diffraction (XRD) and neutron powder diffraction indicated a tetragonal structural transformation at  $T_N$ , subsequent neutron and synchrotron radiation results on single crystal showed an orthorhombic phase.<sup>13-15</sup> Moreover, recent neutron powder diffraction found no sign of structural transition.<sup>10</sup> In fact, the exact lattice symmetry is still subject of debate. On the other hand, IR spectroscopy experiment reported a marked splitting of the low-frequency mode below  $T_N$ .<sup>16</sup> This elucidates an essential spin-phonon coupling. Both geometrical and additional bond frustration are believed to be crucial factors.<sup>6,17</sup> In addition, since  $\text{Cr}^{3+}$  in an octahedral crystal field is Jahn-Teller inactive, spin-phonon coupling is of vital importance in lifting frustration. Moreover, the correlation between spin and lattice

degrees of freedom is also revealed by the recent ultrasonic experiments.<sup>18</sup> Nevertheless, the very origin of NTE is yet far from being well understood.

In the present paper, a set of experimental techniques is utilized to probe the spin-lattice correlation in  $\text{ZnCr}_2\text{Se}_4$ . By considering a variable exchange integral  $J$  with respect to temperature or lattice constant, NTE is attributed to a result of the competition between magnetic exchange and lattice elastic energy via magnetoelastic coupling.

### II. EXPERIMENTS

The polycrystalline sample of  $\text{ZnCr}_2\text{Se}_4$  was prepared by standard solid state reaction method. High purity powders of zinc (99.9%), chromium (99.9%), and selenium (99.9%) were mixed according to the stoichiometric ratio. Next, the powders were sealed in an evacuated quartz tube and heated slowly to  $850^\circ\text{C}$  in seven days. Then the sample was reground, pelletized, sealed, and heated again for another three days at  $850^\circ\text{C}$ . The magnetic data were collected on a Quantum Design superconducting quantum interference device (SQUID) magnetometer. The temperature dependent XRD patterns were obtained using XRD (Rigaku TTRIII). ESR measurements were performed using a Bruker EMX plus 10/12 CW-spectrometer at X-band frequencies ( $\nu=9.39$  GHz) in a continuous He gas-flow cryostat for 2–300 K. The transmittance spectra were collected in the far-infrared range using the Bruker Fourier-transform spectrometer Vertex 80v equipped with a He bath for 5–300 K.

### III. RESULTS AND DISCUSSION

The XRD data were analyzed using the standard Rietveld technique, which shows a single-phase material with cubic spinel structure at room temperature. Figure 1(a) shows the temperature ( $T$ ) dependence of lattice constant  $a$ . With decreasing temperature,  $a$  first decreases rapidly and then manifests a negative thermal expansion behavior below about  $T_E=60$  K, which is almost concordant with the previous results.<sup>6,10</sup> Upon further cooling below 20 K, splitting of

<sup>a)</sup>Author to whom correspondence should be addressed. Electronic mail: zryang@issp.ac.cn.

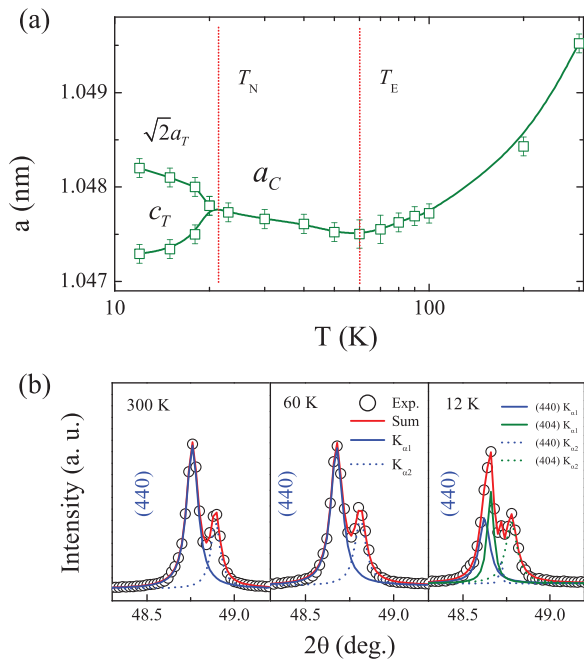


FIG. 1. (a) Temperature dependent lattice parameter  $a$  vs  $T$  in semilogarithmic for  $\text{ZnCr}_2\text{Se}_4$ . Error bars are average of repeated fittings. The negative thermal expansion initial temperature  $T_E$  and the antiferromagnetic order one  $T_N$  are drawn in red dotted lines. (b) The representative peaks (440) at 300 K, 60 K, and 12 K. Circles are experimental data; Solid and dashed lines are Lorentzian fits.

several peaks in XRD spectra are observed. The representative peak (440) at 12 K that splits into (440) and (404) is presented in Fig. 1(b). This signals a cubic to tetragonal structural transition with space group  $I4_1/amd$ .<sup>13,15</sup>

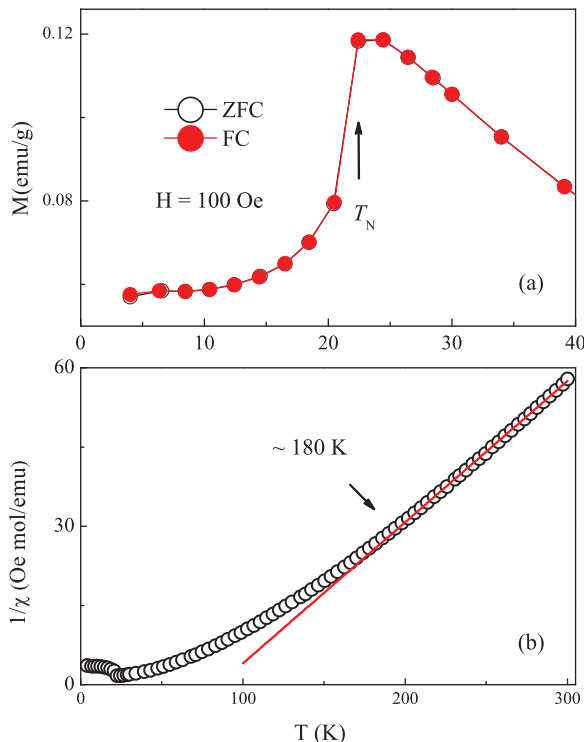


FIG. 2. (a) Low temperature dependence of the magnetization  $M$  for a polycrystalline sample  $\text{ZnCr}_2\text{Se}_4$  at 100 Oe. (b) A Curie-Weiss fitting of the inverse susceptibility.

Figure 2(a) presents the magnetization ( $M$ ) versus  $T$  at low applied magnetic field of 100 Oe under both zero-field-cooled (ZFC) and field-cooled (FC) sequences. At about  $T_N = 22$  K,  $M$  shows a sharp antiferromagnetic (AFM) transition.<sup>6,10,12–14</sup> Figure 2(b) shows a fitting of the inverse susceptibility  $1/\chi$  according to the paramagnetic (PM) Curie-Weiss law  $\frac{1}{\chi} = \frac{T - \Theta_{\text{CW0}}}{C}$ . A large positive Curie-Weiss temperature  $\Theta_{\text{CW0}} = 85$  K and the coefficient  $C = 3.74$  are obtained. The effective magnetic moment calculated by the formula  $\mu_{\text{eff}} = 2.83\sqrt{C/2}$  (in cgs units) equals to  $3.87 \mu_B$ , in agreement with the spin-only  $\text{Cr}^{3+}$  ion.

The large positive Curie-Weiss temperature implies a dominant FM exchange interaction; however, the compound shows an AFM ordering at low temperatures. Hence, we first investigate the lattice dynamic inspired by the strong spin-lattice correlation. Within the wave-number range inspected, three infrared modes, labeled as *I*, *II*, and *III* are observed simultaneously. Generally speaking, the phonon eigenfrequency follows an anharmonic behavior, which can be described by the following formula:

$$\omega_i = \omega_{0i} \left[ 1 - \frac{\alpha_i}{\exp(\Theta/T) - 1} \right], \quad (1)$$

where  $\omega_{0i}$ ,  $\alpha_i$ , and  $\Theta$  are the eigenfrequency of mode  $i$  with decoupling of the spin and phonon at 0 K, the weight factor of mode  $i$ , and the Debye temperature  $\Theta = 309$  K.<sup>16</sup> A detailed temperature dependence of eigenfrequency is exhibited in Fig. 3. The solid line is a fitting of classical anharmonic behavior according to Eq. (1). Mode *I* shows negative shifts below  $T_E$  and Mode *II* shows positive shifts from about 100 K compared to the normal anharmonic behaviors, respectively. According to Lutz and Zwinscher, the highest

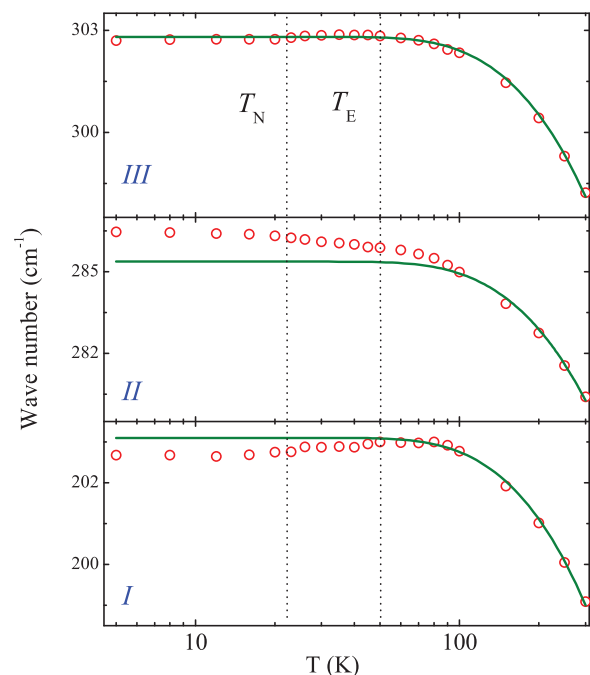


FIG. 3. Temperature dependence of wave number of the infrared activated mode *I*, *II*, and *III* for  $\text{ZnCr}_2\text{Se}_4$ . The solid curve is a fit described in the text. The characteristic temperatures are indicated.

frequency mode III is ascribed to the Cr-Se vibration, however, modes II and I originate from combined vibrations of Cr-Se and Zn-Se. For mode II, the ratio of contribution from Cr-Se and Zn-Se is 78:18, while for mode I the ratio of Cr-Se to Zn-Se is 21:73.<sup>19</sup> Cr-Se bond relates to the FM spin super-exchange interaction and Zn-Se links to the AFM super-exchanges.<sup>4</sup> As a result, FM Cr-X-Cr bonds dominate modes II and III while AFM linkages Cr-X-A-X-Cr determine mainly the eigenfrequency of mode I.<sup>20,21</sup> The deviation of mode II below 100 K due to spin-phonon coupling indicates that FM fluctuations involve already at this temperature. Furthermore, the opposite shifts of modes I and II in the NTE temperature region may refer to a dynamic competition of FM and AFM superexchanges.

The temperature dependent ESR spectrum is further investigated. A PM signal is observed at room temperature and it vanishes below  $T_N$  (not drawn). The resonant field ( $H_{\text{res}}$ ) and peak-to-peak line-width ( $\Delta H_{\text{pp}}$ ) as a function of temperature are plotted in Figs. 4(a) and 4(b), respectively. A typical ESR spectrum at 100 K and fitting using the first-order derivative symmetric Lorentzian function are presented in the inset of Fig. 4(a). As can be seen from Fig. 4(a), with decreasing temperature from 300 K to 100 K,  $H_{\text{res}}$  shows a constant value while  $\Delta H_{\text{pp}}$  decreases almost linearly. Upon further cooling,  $H_{\text{res}}$  drops drastically and accordingly  $\Delta H_{\text{pp}}$  broadens greatly, in accordance with Ref. 6.

The  $g$  factor is 1.996, in agreement well with the previous works.<sup>6,22,23</sup> The linear decrease of  $\Delta H_{\text{pp}}$  with temperature can be attributed to a single-phonon spin-lattice relaxation mechanism.<sup>24,25</sup> Both the constant  $g$ -factor and

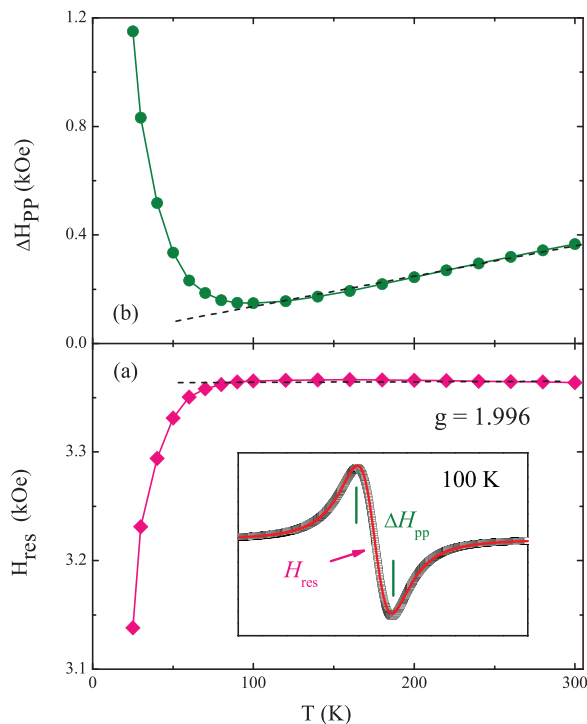


FIG. 4. (a) Temperature dependence of the resonance field  $H_{\text{res}}$ . Inset: a typical fitting of the ESR spectrum at 100 K, where the definitions of the parameters are shown. (b) The peak-to-peak linewidth  $\Delta H_{\text{pp}}$  vs  $T$ . The dashed lines are guided by eyes.

linear behavior of  $\Delta H_{\text{pp}}$  evidence a well-defined PM state at least above 100 K. Note that  $H_{\text{res}}$  starts to decrease and  $\Delta H_{\text{pp}}$  broadens at 100 K. Meanwhile, an FM-related positive shift for Mode II is observed in the IR modes in Fig. 3. These can thereby be correlated to the onset of FM fluctuations and spin-phonon coupling. As we know,  $H_{\text{res}}$  is a sum of  $H_{\text{int}}$  and  $H_{\text{ext}}$ , where  $H_{\text{int}}$  and  $H_{\text{ext}}$  are the equivalent internal and the external actual fields, respectively. For the case  $H_{\text{int}} > 0$ , the internal field may shift the resonance line to lower field; on the contrary, the resonance signal would appear at higher field with negative internal magnetic field. The decreasing of  $H_{\text{res}}$  below 100 K indicates an increasing of  $H_{\text{int}}$ , which may be caused by the interaction between the localized magnetic moments and the demagnetization effect.<sup>24</sup> Therefore, the enhancement of  $H_{\text{int}}$  and onset of FM fluctuations reveal gradually growing FM clusters, forming an FM-cluster and PM mixed state from 100 K to  $T_N$ . The existence of FM clusters is also supported by the following NTE analysis. Below  $T_N$ , the signal disappears due to the AFM ordering transition.

As is discussed above, the system keeps a pure PM state at least above 100 K, so the inverse susceptibility should be described by the PM Curie-Weiss law down to this temperature. However, it departs from the linear behavior at a temperature as high as about 180 K, see Fig. 2(b). Recalling the fitting process in Fig. 2(b), we have assumed a constant Curie-Weiss temperature  $\Theta_{\text{CW}0}$ , i.e., a constant magnetic exchange interaction  $J$ . The behavior of IR modes below 100 K implies a competition of FM and AFM superexchange interactions. In addition, the nearest neighbor FM Cr-Se-Cr and other neighbor AFM Cr-Se-Zn-Se-Cr superexchange interactions depend strongly on the lattice constant.<sup>4</sup> It means that the total  $J$  may change since  $a$  decreases dramatically upon cooling [Fig. 1(a)]. Accordingly, the traditional Curie-Weiss behavior should be modified within the present case to bridge the gap mentioned above. In specific, one should take a variable  $\Theta_{\text{CW}}$  (or  $J$ ) as a function of  $T$  or  $a$  into account.

In AFM spinel oxides, the Curie-Weiss temperature changes exponentially with the lattice parameter.<sup>20</sup> Naturally, an empirical description of  $\Theta_{\text{CW}}(T) = \Theta_{\text{CW}0} - \alpha \times e^{-T/\beta}$  is postulated. The fitting of the inverse susceptibility above 100 K using the modified Curie-Weiss behavior  $\frac{1}{\chi} = \frac{T - \Theta_{\text{CW}}(T)}{C}$  is exhibited in Fig. 5(a). The parameters are  $\alpha = 226$  and  $\beta = 45$ . Furthermore, a remarkable deviation below 100 K in blue short dashed line indicates the appearance of the effective internal field originating from FM clusters. Next, based on the obtained  $\alpha$  and  $\beta$ ,  $\Theta_{\text{CW}}(T)$  is extrapolated to low temperatures as exhibited in Fig. 5(b). It shows a derivation at about 180 K from the nearly constant value. With further lowering temperature, it decreases faster and faster and below  $T \approx 45$  K,  $\Theta_{\text{CW}}(T)$  even becomes negative. These features may interpret qualitatively the fact that  $\text{ZnCr}_2\text{Se}_4$  is dominated by ferromagnetic exchange interaction but orders antiferromagnetically at low temperatures. Since the exchange integral and the Curie-Weiss temperature are linked by  $J(T) \propto \Theta_{\text{CW}}(T)$  [ $J(a) \propto \Theta_{\text{CW}}(a)$ ], we will use  $J(T)$  [ $J(a)$ ] instead in the following discussion.

Given that  $J$  is changeable, magnetic exchange and lattice elastic energies can link effectively with each other via

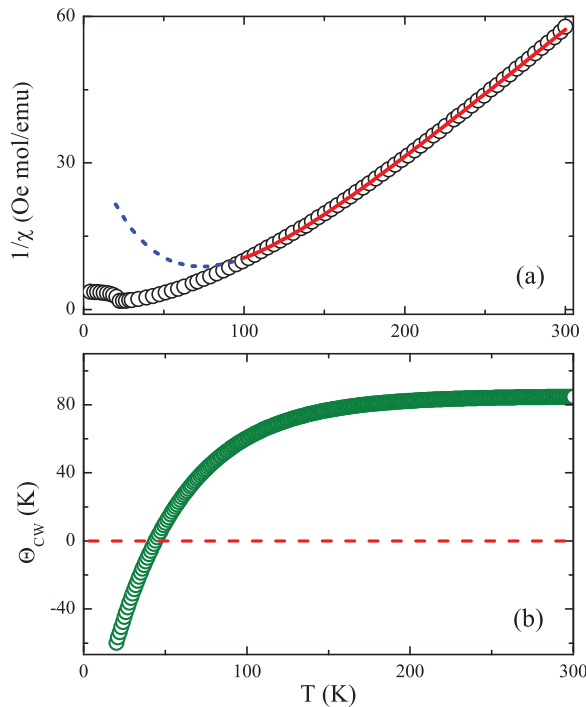


FIG. 5. (a) A fitting of the inverse susceptibility above 100 K in red solid line using  $\frac{1}{\chi} = \frac{T - \Theta_{CW}(T)}{C}$  taking a temperature or lattice constant  $a$  dependent Curie-Weiss temperature into account. The short dashed blue line is an extension of the fitting to low temperatures. (b)  $\Theta_{CW}$  vs  $T$  and the red dashed line indicates  $\Theta_{CW} = 0$  at 45 K.

magnetoelastic coupling. The free energy  $F$  in a magnetoelastic system is expressed as

$$F(T) = -J(T) \sum_{ij} \vec{S}_i \cdot \vec{S}_j + \frac{1}{2} N \omega^2 \Delta^2(T) - T \cdot S(T), \quad (2)$$

where  $N$  is the number of the ion sites,  $\omega$  is the averaged vibrational angular frequency, and  $\Delta$  is the averaged strain relative to the equilibrium lattice constant. The first term is exchange energy ( $E_{ex}$ ) as a function of  $J$ , the second is lattice elastic energy ( $E_{el}$ ) related mainly to the lattice parameter  $a$  (or equivalent  $T$ ), and the last is the entropy. From the above equation, we know that if the system stays at an ideal PM state, then  $E_{ex} = 0$ . So  $E_{ex}$  and  $E_{el}$  will show no coupling, as is observed from the IR spectra above 100 K.

When the system stays at an FM state with a changeable  $J$ , there may exist a competition between  $E_{ex}$  and  $E_{el}$  since the former is negative while the latter always positive. Indeed, it has been concluded above that  $J$  decreases exponentially [Fig. 5(a)] and some FM clusters forms gradually below 100 K. Therefore, the concomitant decrease of  $J$  and  $a$  causes an increasing  $E_{ex}$  but decreasing  $E_{el}$  in the FM clusters. At some critical point, a totally compensation between them may present. If  $a$  further decreases as cooling, the variation of  $E_{ex}$  would gradually exceed that of  $E_{el}$  in magnitude. Especially when  $J$  drops sharply with respect to  $a$ , say here at  $T_E$ , a tiny decrement of  $a$  will give rise to a dramatic increment of  $E_{ex}$  whereas  $E_{el}$  keeps nearly constant. The state in a system subjected to stimuli, such as cooling, always tends to develop towards one that can lower  $F$ . In this sense it is favorable to lowering  $F$  by expanding the lattice parameter  $a$

to increase  $J$  ( $J > 0$ ), and thereby to decrease  $E_{ex}$  due to its negative value, at the same time at a cost of few increases of  $E_{el}$  in magnitude. This means that a negative thermal expansion of the lattice originating from the FM clusters with an exponentially changeable  $J$  is expected. It is worthy of noting that when applying a magnetic field to the system in the NTE temperature region, NTE in magnitude enhances.<sup>6</sup> This is because the size or population of the FM clusters increases when applying a magnetic field.

On the contrary, when an AFM ordering appears,  $J$  becomes negative and the condition to stimulate NTE is not met any more. Normal thermal expansion upon cooling results in a simultaneous decreasing of  $E_{ex}$  and  $E_{el}$ , which is consistent to lowering  $F$ . In fact, a normal expansion feature is observed below  $T_N$ .<sup>6</sup> It should be noted that the existence of NTE<sup>6,10</sup> evidences in turn that  $J$  is changeable. If  $J$  keeps constant in a FM cluster,  $E_{ex}$  will be almost constant and a normal thermal expansion of the lattice alone can give rise to a decrease of  $E_{el}$  and of  $F$  sufficiently.

#### IV. CONCLUSIONS

To summarize, we have investigated the origin of NTE in strongly bond frustrated  $\text{ZnCr}_2\text{Se}_4$ . By fitting the inverse susceptibility above 100 K, an exponentially variable exchange  $J$  is deduced. The exchange and lattice elastic energy can effectively couple with each other via magnetoelastic on basis of this changeable  $J$ . NTE is qualitatively interpreted as a competition between the two kinds of energy.

#### ACKNOWLEDGMENTS

This research was financially supported by the National Key Basic Research of China Grant Nos. 2010CB923403 and 2011CBA00111, and the National Nature Science Foundation of China Grant No. 11074258.

<sup>1</sup>J. S. Gardner, M. J. P. Gingras, and J. E. Greedan, *Rev. Mod. Phys.* **82**, 53 (2010).

<sup>2</sup>L. Balents, *Nature* **464**, 199 (2010).

<sup>3</sup>R. Tong, Z. R. Yang, C. Shen, X. B. Zhu, Y. P. Sun, L. Li, S. L. Zhang, L. Pi, Z. Qu, and Y. H. Zhang, *EPL* **89**, 57002 (2010).

<sup>4</sup>P. K. Baltzer, P. J. Wojtowicz, M. Robbins, and E. Lopatin, *Phys. Rev.* **151**, 367 (1966).

<sup>5</sup>L. Q. Yan, J. Shen, Y. X. Li, F. W. Wang, Z. W. Jiang, F. X. Hu, J. R. Sun, and B. G. Shen, *Appl. Phys. Lett.* **90**, 262502 (2007).

<sup>6</sup>J. Hemberger, H.-A. Krug von Nidda, V. Tsurkan, and A. Loidl, *Phys. Rev. Lett.* **98**, 147203 (2007).

<sup>7</sup>I. Kim, Y. S. Oh, Y. Liu, S. H. Chun, J.-S. Lee, K.-T. Ko, J.-H. Park, J.-H. Chung, and K. H. Kim, *Appl. Phys. Lett.* **94**, 042505 (2009).

<sup>8</sup>K. Siratori and E. Kita, *J. Phys. Soc. Jpn.* **48**, 1443 (1980).

<sup>9</sup>H. Murakawa, Y. Onose, K. Ohgushi, S. Ishiwata, and Y. Tokura, *J. Phys. Soc. Jpn.* **77**, 043709 (2008).

<sup>10</sup>F. Yokaichiya, A. Krimmel, V. Tsurkan, I. Margiolaki, P. Thompson, H. N. Bordallo, A. Buchsteiner, N. Stüßer, D. N. Argyriou, and A. Loidl, *Phys. Rev. B* **79**, 064423 (2009).

<sup>11</sup>F. K. Lotgering, in *Proceedings of the International Conference on Magnetism, Nottingham, 1964* (Institute of Physics and the Physical Society, London, 1965), p. 533.

<sup>12</sup>R. Plumier, *J. Physiol. (Paris)* **27**, 213 (1966).

<sup>13</sup>J. Akimitsu, K. Siratori, G. Shirane, M. Iizumi, and T. Watanabe, *J. Phys. Soc. Jpn.* **44**, 172 (1978).

- <sup>14</sup>M. Hidaka, N. Tokiwa, M. Fujii, S. Watanabe, and J. Akimitsu, *Phys. Status Solidi B* **236**, 9 (2003).
- <sup>15</sup>R. Kleinberger and R. de Kouchkovsky, *C.R. Acad. Sci. Paris, Ser. B* **262**, 628 (1966).
- <sup>16</sup>T. Rudolf, Ch. Kant, F. Mayr, J. Hemberger, V. Tsurkan, and A. Loidl, *Phys. Rev. B* **75**, 052410 (2007).
- <sup>17</sup>S.-H. Lee, C. Broholm, W. Ratcliff, G. Gasparovic, Q. Huang, T. H. Kim, and S. W. Cheong, *Nature (London)* **418**, 856 (2002).
- <sup>18</sup>V. Felea, S. Yasin, A. Günther, J. Deisenhofer, H.-A. Krug von Nidda, S. Zherlitsyn, V. Tsurkan, P. Lemmens, J. Wosnitzer, and A. Loidl, *Phys. Rev. B* **86**, 104420 (2012).
- <sup>19</sup>J. Zwinscher and H. D. Lutz, *J. Alloys Compd.* **219**, 103 (1995).
- <sup>20</sup>T. Rudolf, Ch. Kant, F. Mayr, J. Hemberger, V. Tsurkan, and A. Loidl, *New J. Phys.* **9**, 76 (2007).
- <sup>21</sup>K. Wakamura and T. Arai, *J. Appl. Phys.* **63**, 5824 (1988).
- <sup>22</sup>J. J. Stickler and H. J. Zeiger, *J. Appl. Phys.* **39**, 1021 (1968).
- <sup>23</sup>K. Siratori, *J. Phys. Soc. Jpn.* **30**, 709 (1971).
- <sup>24</sup>C. Rettori, D. Rao, J. Singley, D. Kidwell, S. B. Oseroff, M. T. Causa, J. J. Neumeier, K. J. McClellan, S.-W. Cheong, and S. Schultz, *Phys. Rev. B* **55**, 3083 (1997).
- <sup>25</sup>D. L. Huber and M. S. Seehra, *J. Phys. Chem. Solids* **36**, 723 (1975).